JGR Oceans

RESEARCH ARTICLE
10.1029/2020JC016152

Key Points:
- Observed pH and Ω in hypoxic water in the nGoM are lower than those estimated from anthropogenic CO_2 increase and organic carbon respiration
- The lower pH and Ω values are caused by neglecting benthic anaerobic respiration
- Benthic anaerobic respiration and subsequent alkalinity removal further increase the susceptibility of coastal waters to ocean acidification

Supporting Information:
- Supporting Information S1

Correspondence to:
W.-J. Cai,
wcai@udel.edu

Citation:
Wang, H., Lehrter, J., Maiti, K., Fennel, K., Laurent, A., Rabalais, N., et al. (2020). Benthic respiration in hypoxic waters enhances bottom water acidification in the northern Gulf of Mexico. *Journal of Geophysical Research: Oceans*, *125*, e2020JC016152. https://doi.org/10.1029/2020JC016152

Received 17 FEB 2020
Accepted 31 AUG 2020
Accepted article online 22 SEP 2020

Benthic Respiration in Hypoxic Waters Enhances Bottom Water Acidification in the Northern Gulf of Mexico

Hongjie Wang[1], John Lehrter[2], Kanchan Maiti[3], Katja Fennel[4], Arnaud Laurent[4], Nancy Rabalais[3], Najid Hussain[1], Qian Li[1], Baoshan Chen[1], K. Michael Scaboo[1], and Wei-Jun Cai[1]

[1]School of Marine Science and Policy, University of Delaware, Newark, DE, USA, [2]Department of Marine Sciences, University of South Alabama, Dauphin Island Sea Laboratory, Dauphin Island, AL, USA, [3]Department of Oceanography and Coastal Sciences, Louisiana State University, Baton Rouge, LA, USA, [4]Department of Oceanography, Dalhousie University, Halifax, Nova Scotia, Canada

Abstract It is known that surface water eutrophication enhances bottom water ocean acidification via respiration in coastal oceans. However, the role of benthic processes in influencing bottom water acidification has not been sufficiently explored. We examined this issue by analyzing a 10-year summer carbonate chemistry dataset in bottom water together with recent benthic flux measurements and literature benthic flux data in the northern Gulf of Mexico. The difference between the observed and estimated pH (Ω) values calculated from anthropogenic CO_2 increase and water column aerobic respiration were defined as ΔpH (ΔΩ). We found that ΔpH and ΔΩ values in hypoxic condition were -0.03 ± 0.04 (mean ± standard deviation) and -0.15 ± 0.39, respectively. Both ΔpH and ΔΩ values in hypoxic conditions were significantly lower than zero ($p < 0.05$). The net results of anaerobic respiration, oxidation of reduced chemcials, burial of iron sulfide minerals, and possible $CaCO_3$ dissolution may have led to an alkalinity to DIC production ratio of less than 1 in porewater. This caused the ratio of alkalinity to dissolved inorganic carbon fluxes from sediment to bottom water to be less than 1, which led to additional bottom water acidification. Our analysis and model simulations demonstrate that severe hypoxic and anoxic conditions, which correspond to less water movement, favor the accumulation of benthic respiration products, leading to additional pH and Ω reductions. The findings on sediment processes contributing to acidification in bottom waters provide new insights into the sensitivity of coastal ocean acidification to low-oxygen conditions under current and future climates and anthropogenic nutrient loading scenarios.

Plain Language Summary The ongoing decrease in seawater pH as a result of uptake of anthropogenic carbon dioxide (CO_2) from the atmosphere is known as ocean acidification, which can be enhanced by oxygen-consuming respiration in the water column. Meanwhile, regions of coastal hypoxia (dissolved oxygen <2 mg L^{-1} or 63 μmol L^{-1}) have increased in size and number during the last several decades because of water column eutrophication. Previous studies take only the anthropogenic CO_2 intrusion and aerobic respiration (respiration that consumes oxygen) into consideration when predicting the water column pH and carbonate mineral saturation. However, we found that anaerobic respiration (respiration that does not consumes dissolved oxygen) and the subsequent alkalinity removal via metal-sulfide burials in sediments can further decrease pH and carbonate mineral saturation. Therefore, the bottom water acidification states are more aggravated in hypoxic conditions than previous estimations in the northern Gulf of Mexico. To our knowledge, this is the first study that uses data from multiple years and systematically examines the role of benthic fluxes on ocean acidification in eutrophic coastal bottom waters. The finding has profound implications for similar coastal systems where eutrophication-induced bottom ocean acidification is likely more severe than we used to think.

1. Introduction

Ocean deoxygenation and ocean acidification (OA) resulting from natural and anthropogenic activities are threatening marine ecosystem health (Doney, 2010; Gruber, 2011). Global warming decreases oxygen solubility and increases stratification and thus is likely to further increase low-oxygen areas (Breitburg et al., 2018; Brewer & Peltzer, 2016; Turner et al., 2017). Biogeochemical models for the northern Gulf of Mexico (nGoM) predict that the hypoxic area (dissolved oxygen, or DO <2 mg L^{-1} or 63 μmol L^{-1}) will increase by 26% between 2000s and ~2100 (Laurent et al., 2018). Also, the duration of hypoxia that

occurs over an annual cycle will also increase (Lehrter et al., 2017). At the same time, increasing nutrient runoff is triggering eutrophication, which enhances production of more organic carbon in the water column (Smith, 2003). When this organic carbon sinks below the pycnocline, microbial respiration leads to the development of hypoxic or anoxic conditions (DO = 0 μmol L^{-1}) in physically isolated bottom waters (Rabalais et al., 1994, 2002). While inorganic carbon uptake by primary production reduces surface water acidification (Borges & Gypens, 2010; Laruelle et al., 2018; Wang et al., 2017), the respiration of organic carbon in both water column and sediment releases CO_2 back to the bottom water and accelerates bottom water acidification (Berelson et al., 2019; Cai et al., 2011; Feely et al., 2010; Hagens et al., 2015; Wallace et al., 2014). In hypoxic or anoxic bottom waters, benthic flux and subsequent oxidation of reduced chemicals may further draw down local pH (pH < 7.5; Cai et al., 2017). Meanwhile, the change of riverine alkalinity and dissolved inorganic carbon inputs from watersheds may either increase or decrease the buffering capacity in coastal systems (Duarte et al., 2013; Salisbury et al., 2008; Van Dam & Wang, 2019). Understanding the interactions among the above processes is crucial to determining current and future coastal ocean acidification states.

Eutrophication results in increased accumulation of labile organic carbon in the surface sediments of the northern Gulf of Mexico (Rabalais, Turner, Gupta, et al., 2007). This is likely happening in coastal oceans on a global scale (Dell'Anno et al., 2002; Turner & Rabalais, 1994; Zhao et al., 2015; Zimmerman & Canuel, 2000). As a result, Turner et al. (2008) hypothesized that benthic DO consumption has increased through time, in step with an increase in nutrient loadings from the Mississippi River watershed. A coupled physical-biological model has also shown that the hypoxia formation in the nGoM is sensitive to benthic DO consumption driven by the vertical flux of organic matter from surface waters (Fennel et al., 2013). In general, the contribution of benthic DO consumption to bottom water DO concentration is negatively related to the hypoxic-layer depth (Fennel & Testa, 2019). For example, on average, the benthic consumption accounts for about 20–33% of the oxygen consumption in the hypoxic layer in the nGoM where the hypoxic-layer depth is only ~ 4 m above the seabed (Fennel & Testa, 2019; Murrell & Lehrter, 2011). In comparison, the benthic consumption only contributed 3% to the total oxygen consumption in the East China Sea where the hypoxic-layer depth is much thicker (~25 m). Therefore, in shallow waters and in waters where there is a pycnocline near the bottom, the bottom DO concentration is expected to be more sensitive to the benthic respiration and physical processes of the bottom boundary layer (Kemp et al., 1992; Laurent et al., 2017; Yu et al., 2015).

Benthic respiration not only consumes DO and generates CO_2, but also affects total alkalinity (TA) depending on the dominant redox processes at a given site; for example, reduction of NO_3^-, Mn-oxide, Fe-oxide, and SO_4^{2-} generates TA while oxidation of NH_3, reduced Mn^{2+} and Fe^{2+}, and H_2S consumes TA (Krumins et al., 2013; Van Cappellen & Wang, 1996). The ratio of benthic TA flux and DIC flux is less than 1 within the 100-m water depth in different continental shelves (Hu & Cai, 2011), while the bulk TA/DIC ratio in the water column is nearly 1.2. Therefore, benthic processes have the potential to further decrease bottom water pH (Berelson et al., 2019).

Recently, Hu et al. (2017) simulated the bottom water pH change based on two benthic DIC flux rates that were reported by Rowe et al. (2002) and a global model-derived TA/DIC of 0.25 (Krumins et al., 2013). However, benthic flux measurements in the nGoM carried out in summer 2011, under strong hypoxia, showed an average TA/DIC of 0.8 (Berelson et al., 2019). Nevertheless, Hu et al.'s (2017) simulation supports the idea that the bottom water pH is sensitive to benthic anaerobic respiration products. The pH data from Hu et al. (2017) were collected in late July 2010, three months after the initiation of the Deepwater Horizon oil spill in mid-April, within a month after above average discharge of the Mississippi River in May and June, and shortly after tropical storm Bonnie. It is unclear whether the lowest pH values (~7.6) observed within the 20-m isobath along Louisiana bight in 2010 are a recurring event or were simply an isolated condition in summer 2010 related to higher river discharge, higher carbon flux or stronger stratification (Rabalais et al., 2018).

An analysis of bottom water CO_2 system dynamics in response to benthic fluxes has not yet been reported. Hence, the objective of this study was to synthesize the effect of benthic processes on bottom water pH in the nGoM. Observations of water column carbonate chemistry, benthic fluxes, and results from a biogeochemical model wereused to analyze the underlying mechanisms of any pH and Ω variability from 2006 to 2017.

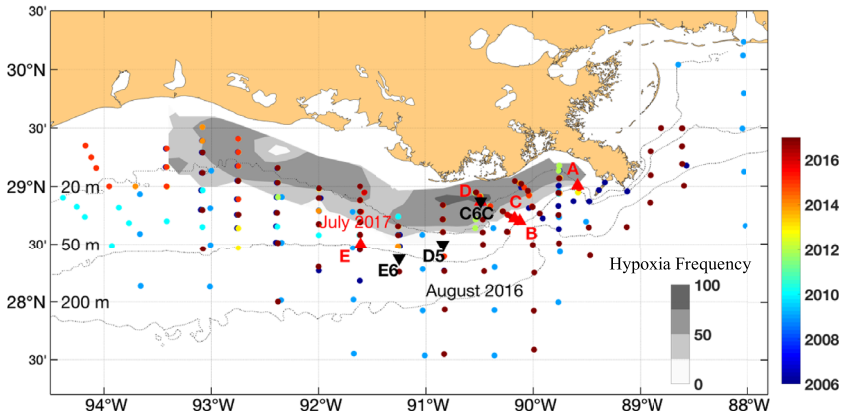

Figure 1. The sampling locations in June, July, August, and September from 2006 to 2017 in the northern Gulf of Mexico. Upward-pointing and downward-pointing triangles represent the stations with sediment incubation in July 2017 and August 2016, respectively. Color map shows the sampling locations in different years from 2006 to 2017. The gray contour or the shaded area shows the frequency of summer bottom water hypoxia based on data collections from 1985 to 2014. Date source: N. Rabalais.

We propose that the physical processes that support the development and maintenance of hypoxia also favor the accumulation of benthic respiration products, leading to further reductions in pH and Ω under prolonged low-oxygen conditions.

2. Data and Methods

2.1. Seawater Carbonate Chemistry

Inorganic carbon data (DIC and TA) were collected from 2006 to 2017 (without 2007 and 2008) on summer cruises (Figure 1 and Table 1), when hypoxia occur red on the Louisiana shelf. The DIC and TA data from 2017 are reported herein. Data previously analyzed and reported include pH and DO data from 2006–2010 and 2017 (Cai et al., 2011; Hu et al., 2017; Jiang et al., 2019), DIC and TA data from 2006 to 2010 (Guo et al., 2012; Hu et al., 2014; Huang et al., 2015), and DIC and DO data from 2011 to 2016 (Wang et al., 2018).

Water samples were taken from Niskin bottles into 250-ml borosilicate glass bottles and were poisoned with 50 μl saturated $HgCl_2$. The samples were kept at 4°C until being analyzed in the laboratory. For DIC, 1 ml of water sample was measured in triplicate with an infrared CO_2 detector-based DIC analyzer (AS-C3 Apollo Scitech). Thereafter, for TA, a 25 ml water sample was measured in duplicate with the open-cell Gran titration method using a temperature-controlled, semi-automated titrator (AS-ALK2 Apollo Scitech). Certified Reference Materials provided by A. G. Dickson, Scripps Institution of Oceanography, were analyzed for DIC and TA for quality control. The precisions for both DIC and TA were within 2 μmol kg^{-1} (±0.1%; Huang et al., 2012). Spectrophotometric pH (pH_{spec}; Liu et al., 2011) was collected in year 2009, 2010, and 2012–2017 (Figure 1 and Table 1). We also calculated pH ($pH_{(TA,\ DIC)}$) and aragonite saturation state (Ω) using the CO2SYS program and the measured DIC and TA as the input pair (van Heuven et al., 2011). Silicate and phosphate concentrations were assigned as 0 in CO2SYS. The coefficients for pH and Ω calculation were selected as: K_1 and K_2 value from Lueker et al. (2000); K_{HF} was from Dickson and Riley (1979);

Table 1
The Inorganic Carbon System Data Collections by Year

	2006	2007	2008	2009	2010	2011	2012	2013	2014	2015	2016	2017
pHspec	N	N	N	Y	Y	N	Y	Y	Y	Y	Y	Y
TA	Y	N	N	Y	Y	Y	Y	Y	Y	Y	Y	Y
DIC	Y	N	N	Y	Y	Y	Y	Y	Y	Y	Y	Y

Note. "N" represents no data collection, while "Y" represents data were collected.

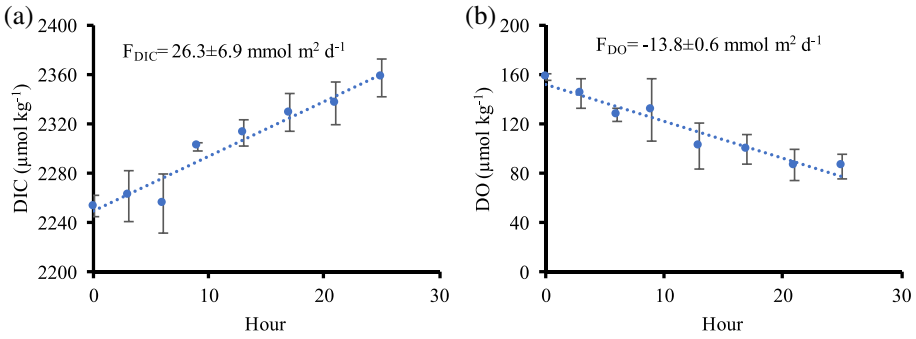

Figure 2. Example concentrations vs. incubation time in Station D for DIC (a) and DO (b) in August 2016. The inserted text shows the calculated final sediment flux (F, mmol m^{-2} d^{-1}). The error bars show the standard deviation of each sampling point ($N = 3$).

K_{HSO4} was from Dickson (1990); and B_T (total boron) was from Uppström (1974). DO was measured by Winkler titration. As noted above, the data used in this study were from summer months (June, July, August, and September) only.

2.2. Benthic Flux Incubation

Sediment-water exchange rates of DO, DIC, and TA were observed at five stations located from the river mouth to the open ocean in August 2016 and July 2017 (Figure 1). In August 2016, Station E, the farthest station from river mouth, was used as a control station outside the regular hypoxic zone. Station A was the closest station from river mouth. Station B was located at the edge of the regular hypoxic zone, while Stations C and D were within the core of the hypoxic zone (Figure 1). Thus, Stations C and D from August 2016 were representative of the hypoxic zone and for estimation of the impact of benthic respiration on the bottom water inorganic carbon system. Station C6C from July 2017 was the same station as Station D from August 2016. Stations D5 and E6 from July 2017 were further offshore and outside of the regular hypoxia area.

At each station, sediments were collected using either a multicorer or a 0.25-m^2 box corer that was subsampled in triplicate with Plexiglas cylindrical chambers (10-cm ID × 40 cm). The overlying water column inside the core incubations collected via multicorer were adjusted to a constant height of 25 cm using custom design lids that can be positioned at any height inside the core tube. For samples collected by box corer, the core tubes were manually inserted into the box corer sample. Immediately after collection, three incubation cores per station were immersed in a temperature-controlled recirculating water bath incubator adjusted to the recorded bottom water temperature. Each core was carefully filled with *in situ* near-bottom water with minimum disturbance to the sediment-water interface and closed to ensure no visible headspace or air bubbles at the top. All cores were attached to a reservoir containing bottom water for gravity driven replenishment of water inside the cores during sampling so as not to introduce any air bubbles. The core incubations were conducted following the method outlined by Lehrter et al. (2012), briefly described below.

Sediment incubations were carried out in triplicate core chambers containing sediments and overlying water plus one control chamber with bottom water only. Incubations occurred in the dark for 16–30 hr, depending on the final DO concentrations (2–3 mg L^{-1} or 63–95 μmol L^{-1}). Water samples in the incubation tubes were collected at regular intervals (e.g., Figure 2). DO was measured at each sampling point using temperature-compensated micro-optodes (Hach LDO101 with Hq40d meter). Samples for DIC and TA were collected in 12-ml exetainers, fixed with saturated $HgCl_2$ and stored at 4–5°C until final analysis. DIC and TA were measured with the same method as for water samples. However, in the case of TA, the water sample volume was reduced. After DIC analysis, about 3 ml of sample was first weighed in a small beaker with an electronic balance, and then 1 ml of DI water was added to the beaker before being titrated with the AS-ALK 2 titration system equipped with a 6 mm diameter Ross combination glass pH electrode. The analytical precision was about ±0.15%. The decline in DO or increase in DIC and TA within an incubation chamber over time was generally monotonic (Figure 2). Therefore, benthic fluxes (mmol m^{-2} d^{-1}) of DO, DIC, and TA were calculated by linear regression of constituent concentrations versus incubation time. Benthic flux rates were

corrected for water column processes by subtracting rates measured in control chambers filled only with bottom water. The regression p value was used to determine if a flux rate was significantly different from zero ($\alpha = 0.2$). Hence, in cases where the p value was higher than 0.2, a flux value of zero was assigned. p values greater than 0.2 were common for the control chambers and resulted in most of the control flux values being assigned a value of zero. For the sediment cores, a few of the individual core chambers had fluxes that were not different than zero, but in averaging triplicates of cores chambers wherein each set of triplicates had at least two cores with significant fluxes, we observed non-zero rates at every station. Positive benthic fluxes indicated a net flux out of the sediments to the bottom water, whereas negative fluxes indicated a net flux from the bottom water into the sediments. Note that the measured benthic DO flux in July 2017 may not have been representative of *in situ* flux because the overlying water used for the incubation was collected at mid-depth instead of at the bottom. However, TA and DIC gradients in sediment porewater develop over a much longer timescale than oxygen gradients and subsurface water column DIC and TA gradients were generally small. Therefore, the benthic TA and DIC fluxes in July 2017 were considered to be unaltered by the overlying water during the short-term duration of the flux experiment.

The sediment flux incubations provide a bulk estimation of respiration but do not provide an exact fraction of contributing aerobic and anaerobic process. Thus, we separated the observed benthic flux into "Net-Aerobic" and "Non-Aerobic" parts for the purpose of quantifying the impact of benthic flux on the water column carbonate chemistry. We define "Net-Aerobic" flux as the sum of aerobic respiration and re-oxidation of reduced species generated from anaerobic processes (Canfield et al., 1993). The "Net-Aerobic" part of benthic respiration alters water column DIC, TA, and DO with the same ratio (at a ratio of 106/−17/−138) as the aerobic respiration in water column. The "Non-Aerobic" part is the difference between observed flux and the "Net-Aerobic" part, including net anaerobic respiration and possibly $CaCO_3$ dissolution. Unlike the "Net-Aerobic" part, the "Non-Aerobic" respiration alters water column DIC and TA values but not DO concentration.

2.3. Model Simulation of pH Changes

To determine how pH evolved because of anthropogenic CO_2 intrusion (from 2006 to 2017) and organic carbon aerobic respiration, we performed the following analysis with the same method reported in Cai et al. (2011). In the present study, we used the same representative surface water conditions as in Cai et al. (2011), which were collected from the July 2007 Gulf of Mexico and East Coast Carbon Cruise (GOMECC-1) in the Gulf of Mexico (Salinity = 36.3, Temperature = 25°C, TA = 2398.1 μmol kg^{-1}). For summer 2006, the dried air fraction (xCO_2) was 381.9 ppm (https://www.esrl.noaa.gov/gmd/ccgg/trends/), so the equilibrated pCO_2 for this water mass was 370.2 μatm. Then the air-equilibrated DIC was calculated as 2,057.2 μmol kg^{-1} by inputting the TA and equilibrated pCO_2 to CO2SYS. Using the same method, but for 2017 when the dried air xCO_2 was 406.5 ppm, and by assuming all other parameters to be constant, the air-equilibrated DIC in 2017 was calculated to be 2,071.1 μmol kg^{-1}. We then added the aerobic respiration to these air equilibrated starting points at Redfield ratios (ΔDO: ΔDIC: ΔTA = −138:106:−17). pH@ 25°C and Ω@ 25°C were calculated with CO2SYS by choosing the new pair of DIC and TA values. We assumed DO at the starting points was also equilibrated with the air. With the same method, the pH-DO and Ω-DO evolutions were simulated for all sampling years (2006 to 2017), pre-industrial era (xCO_2 of 280 ppm), and year of 2100 (xCO_2 of 800 ppm).

When quantifying the benthic impact on bottom water pH or Ω changes, we first converted the benthic DO, DIC, and TA fluxes into the concentration changes by dividing the benthic fluxes with the bottom water depth. Then we added the concentration changes to the previous water column DO, DIC, and TA concentrations to get a new set of values. The simulation was stopped after anoxia in water column lasting for 10 days. Eventually, we recalculated the pH@ 25°C and Ω@25°C with benthic impact using CO2SYS (van Heuven et al., 2011).

2.4. Modeled Time-Integrated Low Oxygen Area

In order to scale benthic flux over the entire hypoxic region, we used a coupled physical-biogeochemical model that was configured for the nGoM (Laurent et al., 2018) to obtain the time-integrated low-oxygen bottom area. The time-integrated area of low bottom water DO was defined as the year-integrated area where bottom DO drops below a certain level. For our analysis, we defined two levels of low bottom water DO:

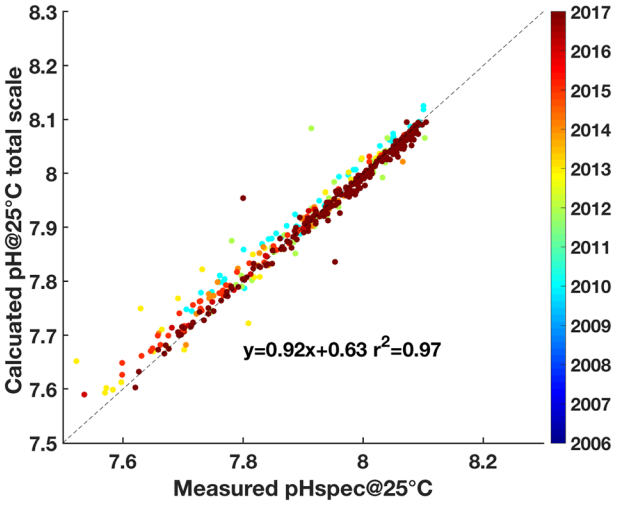

Figure 3. Internal consistency of the inorganic carbon system from 2006 to 2017 (June, July, August, and September) in the northern Gulf of Mexico.

hypoxia (DO < 63 μmol L^{-1}) and severe hypoxia (DO < 30 μmol L^{-1}). For example, the modeled year-integrated hypoxic area in 2017 was estimated to be ~1,932 × 10^3 km^2 yr^{-1} (i.e., the area under the curve in supporting information Figure S1). Time-integrated areas of low bottom water DO represent the cumulative impact of all processes from both water column and sediment before the low DO water was fully abated by loss of stratification or lateral advection of normoxic waters.

3. Results

3.1. Interannual Variability of Bottom Water pH and Ω

We compared pH calculated from DIC and TA with the measured spectrophotometric pH (pH_{spec}) from a subset of cruises and found that the calculated pH was close to the pH_{spec} (Figure 3). The difference between these two datasets was 0.00 ± 0.02, which is within the uncertainty of the pH calculation (Woosley et al., 2017). Therefore, this study adopted the calculated pH and Ω to ensure the longest data record. Further, we only used data points collected from water depth between 12 and 50 m and salinity >32 to best cover the hypoxic area, to achieve spatial consistency across the summer cruises and to reduce the complexity involving surface and bottom mixing in shallow waters (Cai et al., 2011; Hu et al., 2017).

Water column pH decreased with declining DO concentration (Figure 4a). Consistent with a previous study (Cai et al., 2011), water column pH generally agreed with estimations derived from anthropogenic CO_2 intrusion and aerobic respiration. Hereafter, we referred to the difference between observed pH or Ω and estimated values caused by anthropogenic CO_2 intrusion and aerobic respiration as "additional pH declines (ΔpH)" or "additional Ω declines (ΔΩ)." The ΔpH values were −0.01 ± 0.06 (mean ± deviation) in the moderate hypoxic conditions (30 μmol L^{-1} < DO < 63 μmol L^{-1}) and −0.04 ± 0.05 in the severe hypoxic conditions (DO < 30 μmol L^{-1}) (Figures 4a and 4b). In contrast, pH in higher DO conditions were close to the estimated lines (0.00 ± 0.04, Figure 4a). Ω was also positively correlated with DO but more curvature occurred at low DO conditions in the relationship (Figure 4c), which is consistent with a previous study (Feely et al., 2018). Similarly, ΔΩ values also increased significantly with DO decrease. For example, ΔΩ values were −0.08 ± 0.47 in the moderate hypoxic conditions, but as low as −0.20 ± 0.30 in the severe hypoxic conditions (Figure 4d). Overall, both ΔpH and ΔΩ values in the hypoxic conditions were significantly lower than zero ($p < 0.05$). The 95% confidence of the ΔpH values were −0.03 to −0.00 and −0.05 to −0.03 for the moderate hypoxia and severe hypoxic conditions, respectively. The 95% confidence of the ΔΩ values were −0.20 to 0.04 and −0.27 to −0.14 for the moderate hypoxia and severe hypoxic conditions, respectively. The 10 years of summer pH and Ω observations (Figures 4a and 4c) indicated strong year-to-year variability. The observed pH and Ω for DO < 63 μmol L^{-1} tended to be lower than the estimated curves, for example, in summer 2017, when the largest ever recorded hypoxic area occurred (Figure 4a, https://gulfhypoxia.net/research/shelfwide-cruise/?y=2017&p=press_release). After combining all these yearly efforts, both ΔpH and ΔΩ values were significantly related to DO concentration (Figures 4b and 4d, $p < 0.001$).

3.2. Benthic Flux

In August 2016, we assumed that respiration in the upper centimeter of the sediments and DO flux were driven by aerobic respiration due to high bottom water DO concentrations at Station A (144 μmol L^{-1}, Table 2). At Station E, the control station outside the regular hypoxic zone, bottom water DO was also high (150.3 μmol L^{-1}). The negative TA flux at this location, that is, directed from the water column (high TA) into the sediments (low TA), indicated the dominance of aerobic respiration in sediment at this location. The mean DO, DIC, and TA fluxes at Stations C and D (the core of the hypoxic zone) were −13.7 mmol m^{-2} d^{-1}, 33.1 mmol m^{-2} d^{-1}, and 9.5 mmol m^{-2} d^{-1}. In July 2017, the benthic DIC and TA fluxes at the hypoxic station (Station C6C) were 24.9 and 10.1 mmol m^{-2} d^{-1}, respectively. Our measured benthic DIC and TA fluxes were close to the benthic flux (41.5 ± 14.0 vs. 32.4 ± 11.7 mmol m^{-2} d^{-1}) measured by Berelson et al. (2019) in the nGoM. Overall, the benthic fluxes from our 2016 and 2017 observations

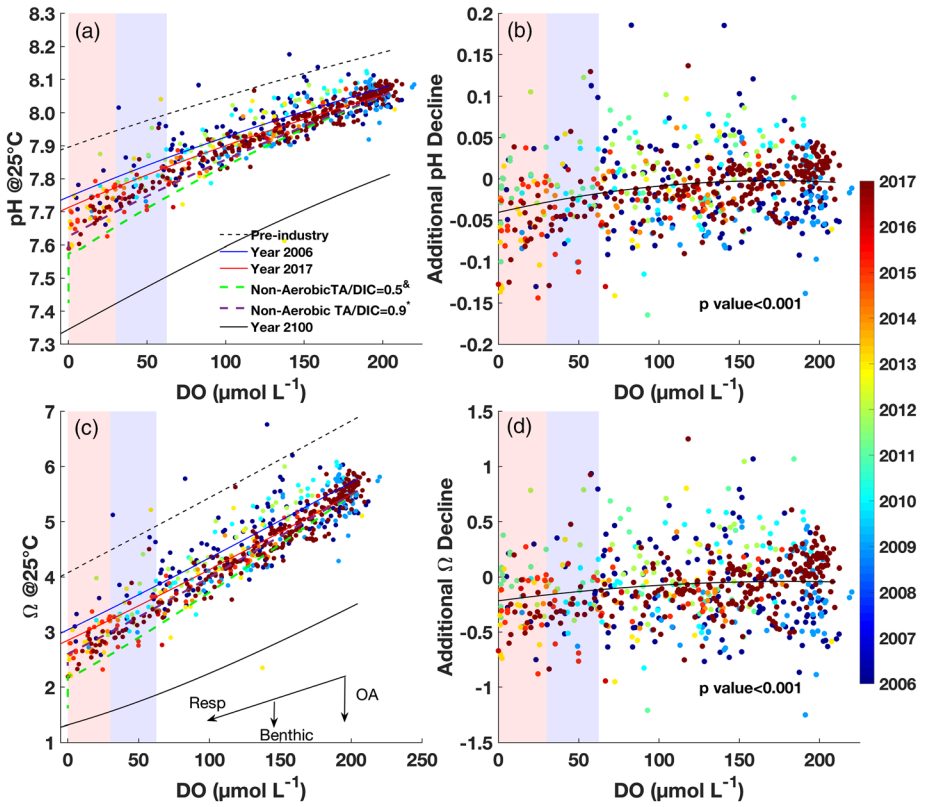

Figure 4. (a) Relationship between pH@25°C and DO from summer 2006 to 2017 in northern Gulf of Mexico. The data presented here are samples collected between 12 and 50 m and with salinity >32. The black dashed, blue, red, and black solid lines represent the pH in the pre-industrial era (xCO_2: 280 ppm), 2006, 2017, and 2100 (xCO_2: 800 ppm) with anthropogenic CO_2 intrusion and aerobic respiration. The green dashed lines (TA/DIC = 0.5) represent the sediment impact simulation based on our August 2016 cruise ($^{\&}$). The purple dashed line (TA/DIC = 0.9) denotes the sediment impact simulation with benthic results from Berelson et al. (2019) (*). The extensions of the green and purple dashed lines are along the zero-oxygen line (*y*-axis) by assuming a 10 days' anoxic conditions. (b) Relation between additional pH decline and DO concentration. Note that additional pH decline is defined as the difference between measured values and estimated ones from aerobic respiration of organic carbon and anthropogenic CO_2 intrusion in water column. The solid line represents the second-order polynomial fit. All notes are the same for panel (c, d) except they are for Ω @25°C, and all panels share the same color bar. pH and Ω changes due to increasing atmospheric CO_2, organic carbon aerobic respiration, and benthic respiration are marked as OA, Resp (respiration) and Benthic in the insert panel c. The shaded purple areas represent the moderate hypoxic conditions (30 μmol L^{-1} < DO < 63 μmol L^{-1}), while red areas highlight the severe hypoxic (DO < 30 μmol L^{-1}) to anoxic (DO = 0 μmol L^{-1}) conditions.

fell within the ranges of other studies in the nGoM (Table 2) and were consistent with an earlier study that found the TA/DIC flux ratio to be less than 1 in other continental shelves such as the Gulf of Cádiz, the Central California shelf/slope, the San Francisco Bay Basin, and the Northern Adriatic Sea summarized by Hu and Cai et al. (2011).

3.3. Benthic Impact Simulations

DO consumption rate in the water column was not measured in August 2016, but a previous shelf wide study by the same authors reported an average water column DO consumption of 6.8 μmol L^{-1} d^{-1} (Murrell & Lehrter, 2011). At this rate, water column aerobic respiration alone should decrease bottom water pH (Ω) from 8.06 to 7.71 (5.56 to 2.86). Note that the interannual or spatial variability of water column DO consumption rate will not impact the stoichiometry of aerobic respiration. Therefore, the variability of water column aerobic respiration will not impact the pH versus DO relationship. It would take 21 days to deplete the saturated DO to zero using the average hypoxic layer depth above the seabed (3.9 m; Obenour et al., 2013), the average measured benthic DO flux from stations C and D in August 2016 (−13.7 mmol m^{-2} d^{-1}, Table 2), and average DO consumption rate in the water column (6.8 μmol L^{-1} d^{-1}). Previous studies also showed

Journal of Geophysical Research: Oceans

10.1029/2020JC016152

Table 2
Summary of DO, DIC, and TA Flux From the Northern Gulf of Mexico (From Our Studies and Those of Others)

Location	Date	Depth	T (°C)	S	DO (μmol L^{-1})
Station A[a]	August 2016	19.5	29.64	31.81	144.7
Station B[a]	August 2016	45.5	24.05	36.32	161.2
Station C[a]	August 2016	35.5	25.80	35.92	132.5
Station D[a]	August 2016	17.5	27.51	33.77	**45**
Station E[a]	August 2016	49.5	24.43	36.08	150.3
Station C6C	July 2017	18.4	16.98	35.12	**26.7**
Station D5	July 2017	31.4	25.23	36.08	173.4
Station E6	July 2017	55.1	22.53	36.21	135.8
Rowe et al. (2002)[b]	July 1991	17.0–21.0 (19.0 ± 1.8)	25.2–26.8 (26.2 ± 0.7)	-	6–83 (26.5 ± 37.7)
Rowe et al. (2002)[b]	April 1992	17–20 (18.5 ± 1.5)	20.0 ± 0.0	-	95–168 (124.5 ± 27.4)
Rowe et al. (2002)[b]	August 1994	12.0–25.0 (20.7 ± 7.5)	27.2–28.6 (28.1 ± 0.8)	-	0–14 (8 ± 7)
Lehrter et al. (2012)[c]	March 2005 to August 2007	5.0–22.0 (13.5 ± 8.3)	20.0–30.0	>35	58.7–125.5 (100 ± 29)
Berelson et al. (2019)[c]	August 2011	18.0–23.0 (21.5 ± 2.4)	22.6–29.2 (25.7 ± 2.7)	25.2–35.8 (32.7 ± 5.0)	0–160 (53 ± 73)

Location	Benthic DO flux (mmol m^{-2} d^{-1})	Benthic DIC flux (mmol m^{-2} d^{-1})	Benthic TA flux (mmol m^{-2} d^{-1})	TA/DIC
Station A[a]	−13.5 ± 0.2	33.0 ± 2.1	−3.3 ± 13.2	−0.1
Station B[a]	−24.6 ± 13.8	33.3 ± 4.2	1.0 ± 3.6	0.03
Station C[a]	−13.7 ± 0.6	39.9 ± 13.3	15.4 ± 21.1	0.39[e]
Station D[a]	−13.8 ± 0.6	26.3 ± 6.9	3.7 ± 9.2	0.14[e]
Station E[a]	−10.9 ± 1.0	84.5 ± 10.5	−15.5 ± 27.8	−0.18
Station C6C	-	24.9	10.1	0.41
Station D5	-	16.0	0.6	0.04
Station E6	-	5.4	2.2	0.40
Rowe et al. (2002)[b]	−18.4 ~ −0.82 (−9.73 ± 7.2)	-	-	-
Rowe et al. (2002)[b]	6–24.5 (19.0 ± 7.5)	14–36 (26.2 ± 9.9)	-	-
Rowe et al. (2002)[b]	−1.9 ~ −56.4 (−25.0 ± 28.2)	24–55 (39.0 ± 15.5)	-	-
Lehrter et al. (2012)[c]	−23.9–0 (−10 ± 6)	7.9–21.5 (17.2 ± 2.4)	-	-
Berelson et al. (2019)[c]	−11.8–0 (−5.1 ± 4.9)	24.8–58.9 (41.5 ± 14.0)	24.2–49.1 (32.4 ± 11.7)	0.57–0.98 (0.80 ± 0.2)[e]

Note. Positive flux is defined as from sediments into the bottom water.
[a]Ebner (2019). [b]Flux data without Station 1 (see details in Rowe et al., 2002). [c]There were no DIC flux measurement in March 2005 (see details in Lehrter et al., 2012). [d]Flux data from entire Gulf of Mexico shelf after excluding Station 8 (see details in Berelson et al., 2019) [e]TA/DIC ratio we used to simulate benthic impact on bottom water pH and Ω (See details in text). The hypoxic stations are highlighted in bold.

that bottom water DO depletion occurs at a similar time scale (Rabalais, Turner, Sen Gupta, et al., 2007). Given that the bottom water currents in the summer nGoM are negligible in the area of high hypoxia frequency (Rabalais et al., 1994; Wiseman et al., 2004), the nearly stagnant bottom water has enough time to be impacted by benthic processes before moving out of hypoxic zone. Using the measured benthic DIC flux from Station C and D (33.1 mmol m^{-2} d^{-1}, Table 2) in August 2016, the total DIC production rate below the pycnocline was 13.7 μmol L^{-1} d^{-1}, which is the sum of water column (5.2 μmol L^{-1} d^{-1}) and benthic respiration rate (33.1/3.9 μmol L^{-1} d^{-1}). With the same approach, the TA production rate below the thermocline was 1.6 μmol L^{-1} d^{-1}. After considering the benthic impact on the bottom water, bottom water pH and Ω under oxygen-free conditions decreased from 8.06 to 7.57, and 5.56 to 2.20, respectively. In other words, with this benthic simulation, we found that benthic respiration could further decrease bottom pH and Ω by 0.14 units and 0.76 units on basis of water column aerobic respiration (Figure 4, green dashed line).

As mentioned above, the shipboard incubations during July 2017 may not be fully representative of the in situ near-bottom conditions because the incubation sediment overlying water used was not truly bottom water, even though the TA and DIC fluxes were considered to be unaltered by the sampling depth (see Section 2.2). Therefore, we did not use July 2017 benthic results to do sediment impact simulation, which required *in situ* benthic DO flux. Using an *in situ* benthic chamber technique, Berelson et al. (2019) found that the average benthic DO, DIC, and TA fluxes across the nGoM were −5.1, 41.5, and 32.4 mmol m^{-2} d^{-1} in August 2011. With this set of benthic fluxes, we found that pH (Ω) decreased from 8.06 to 7.63 (5.56 to 2.63) when bottom water DO was depleted to zero (Figures 4a and 4c, purple line). The additional pH and Ω declines were comparable to the simulations from our own benthic data (Figures 4a and 4c, green line).

3.4. Relationship Between Bottom Water Ocean Acidification and Hypoxic Area

Both modeled hypoxic and severe hypoxic areas varied annually (Figure 5). The mean ΔpH and ΔΩ values in hypoxic conditions were inversely related to the modeled time-integrated hypoxic area (Figure 5b). The greater modeled time-integrated hypoxic and severe hypoxic areas during 2014–2017 resulted in additional pH declines (−0.04 ± 0.00, Figure 5a) versus 0.00 ± 0.01 from 2010 to 2012. Similarly, the annual mean ΔΩ values from 2014 to 2017 were −0.24 ± 0.03, which was more negative than the values from 2010 to 2012 (−0.06 ± 0.10).

4. Discussion

4.1. Benthic Processes Affecting Bottom Water pH and Ω

Benthic fluxes of DO, DIC, and TA are a net result of aerobic and anaerobic processes, which are not homogeneously distributed in the nGoM area of hypoxia. Among them, the benthic DO flux rate covaries strongly with bottom water DO concentration with rates approaching zero when the overlying DO is depleted to zero (Cai & Sayles, 1996; Lehrter et al., 2012; Morse & Eldridge, 2007; Nunnally et al., 2013; Rowe et al., 2002). The mean benthic DO flux in 2016 was −15.3 ± 5.3 mmol m^{-2} d^{-1}, which was almost three times the rate observed by Berelson et al. (2019) in 2011 (−5.1 ± 4.9 mmol m^{-2} d^{-1} when a much lower overlying DO concentration was reported; Table 2). The TA/DIC ratio was low under DO-rich and high benthic DO flux condition. For example, the TA and DIC fluxes at Station B in August 2016 was 1.0 mmol m^{-2} d^{-1} and 33.3 mmol m^{-2} d^{-1}, when the benthic DO flux was −24.6 mmol m^{-2} d^{-1}. The benthic fluxes at this station were likely dominated by aerobic respiration.

Aerobic respiration stops in both water column and sediment when DO concentration approaches zero. Under these suboxic and anoxic conditions, benthic anaerobic respiration proceeds according to the free energy of alternative electron-accepting processes, that is, denitrification, manganese- and iron-oxides reduction, sulfate reduction, and methanogenesis. Remineralization rates of organic matter due to denitrification are often less than rates of manganese- and iron-oxides reduction. The latter two processes are the dominant anaerobic processes in the upper 10 cm of sediment cores across the nGoM shelf (Devereux et al., 2015, 2019). Manganese- and iron-oxides reduction and sulfate reduction all increase TA at a faster rate than DIC (Cai et al., 2010). In addition, $CaCO_3$ dissolution contributes to a TA/DIC ratio of 2:1. In summary, anaerobic respiration and possible $CaCO_3$ dissolution can cause a higher TA/DIC ratio than the one caused by aerobic respiration in sediment.

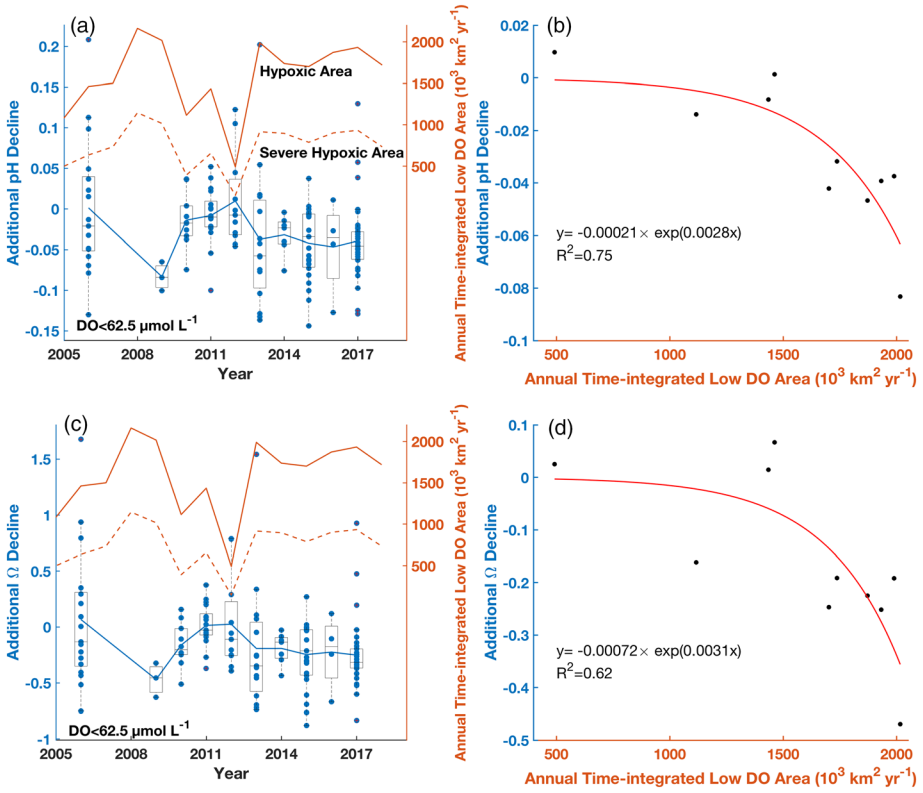

Figure 5. (a) Distribution of additional pH declines at DO < 63 μmol L^{-1} conditions (blue points), modeled time-integrated hypoxic area (<63 μmol L^{-1}, connected orange line), and time-integrated severe hypoxic area (<30 μmol L^{-1}, dashed orange line) over time. The light-gray boxplots show the distribution of additional pH declines in hypoxic water (<63 μmol L^{-1}) or the shaded area in Figure 4 in each year. The blue line connects the mean additional pH declines in each year. (b) Relationship between the mean additional pH declines at DO < 63 μmol L^{-1} and modeled time-integrated hypoxic area. The inserted text shows the best-fit exponential equation. The exponential fitting was selected because it had a higher R^2 than a linear regression (R^2 = 0.64 for pH; R^2 = 0.39 for Ω). All notes in (c, d) are the same as panel (a, b) except they are for additional Ω declines. Note, additional pH or Ω declines mean the difference between measured values and estimated values from organic carbon aerobic respiration and anthropogenic CO_2 intrusion in water column.

Even though the anaerobic processes increase TA in sediments, the subsequent re-oxidation of the reduced species (diagenetic byproducts such as NH_4^+ and H_2S) by O_2 should release H^+ and eliminate the earlier TA increase with a net result equivalent to the aerobic respiration (Canfield et al., 1993). However, the two processes can be decoupled spatially and temporally forming pH maximum and minimum zones in sediment porewater (Cai et al., 2006; Cai & Reimers, 1993). This can be further complicated when there is FeS and FeS_2 formation, which can be buried in sediments without readily being re-oxidized by O_2. It is possible there may be periods, such as summer, when anaerobic processes dominate, and reduced species build up in the sediments (Devereux et al., 2015). These reduced species may not be re-oxidized until fall/winter when DO is replenished (Eldridge & Morse, 2008), so there would be a period when TA is being generated and then later being consumed.

Under low DO conditions in bottom water, benthic DO flux can go to zero while DIC fluxes may be maintained at similar levels as under oxic conditions; thus, most of the DIC is produced through anaerobic processes (Lehrter et al., 2012). The sediment sulfate reduction rate ranges from 17 to 40 mmol m^{-2} d^{-1} (Devereux et al., 2015; Morse & Eldridge, 2007; Rowe et al., 2002). However, the H_2S concentration in the top 15 cm is negligible (Morse & Rowe, 1999). Thus, the majority of produced H_2S must react with metal oxides and be buried in the sediment to maintain very low H_2S concentrations (Leslie et al., 1990; Morse & Eldridge, 2007). We can do a simple estimation to examine the importance of FeS formation and burial in

Table 3
The Summary of Mean DO Conditions, Benthic DO, DIC, and TA Fluxes in August 2016 and August 2011 in the Northern Gulf of Mexico

		Observed benthic flux (mmol m^{-2} d^{-1})			"Net-Aerobic" flux[a] (mmol m^{-2} d^{-1})			"Non-Aerobic" flux[b] (mmol m^{-2} d^{-1})			
DO concentration (μmol L^{-1})		DO	DIC	TA	DO	DIC	TA	DO	DIC	TA	"Non-Aerobic" TA/DIC ratio
August 2016[c]	89	−13.8	33.1	9.6	−13.8	10.6	−1.7	0	22.5	11.2	0.5
August 2011	53	−5.1	41.5	32.4	−5.1	3.9	−0.6	0	37.6	33.0	0.9

[a]"Net-Aerobic" flux is the sum of aerobic process and re-oxidation of reduced species generated from anaerobic processes. For example, the "Total Aerobic" DIC flux in August 2016 was calculated as $-13.8 \times (-106/138) = 10.6$ mmol m^{-2} d^{-1}. [b]"Non-Aerobic" flux is the difference between observed benthic flux and "Net-Aerobic" flux. [c]The benthic fluxes in August 2016 are the average value of Stations C and D, which are within the core of the hypoxic zone.

sediment TA balance. Assuming all the benthic DIC (41.5 mmol m^{-2} d^{-1}) was produced through iron-oxides reduction as described in the below reaction,

$$(CH_2O)_{106}(NH_3)_{16}H_3PO_4 + 4 \times 106FeOOH + 8 \times 106H^+ \Rightarrow 106CO_2 + 4 \times 106Fe^{2+} + 16NH_3 + H_3PO_4$$

with an TA/DIC ratio of $(8 + 16/106 - 1/106) = 8.142$, the sediment could produce a maximum TA as high as 337.9 mmol m^{-2} d^{-1} (41.5 mmol m^{-2} d^{-1} × 8.142). If 90% of produced Fe^{2+} were precipitated as FeS, then 298.8 mmol m^{-2} d^{-1} of previously produced TA could be removed (41.5 mmol m^{-2} d^{-1} × 8 × 90%). Under this extreme scenario, the net TA flux would be 39 mmol m^{-2} d^{-1}, and the TA/DIC ratio in the benthic products would be 0.94. The exact reactions and their ability to cause the observed TA/DIC ratio (<1) are beyond the scope of this study, but our simple scenario analysis indicates that FeS formation is an important process to remove benthic TA. In summary, the combination of anaerobic process, oxidation of reduced species, and iron sulfide precipitation are all important for maintaining an observed benthic TA/DIC ratio (<1).

To quantify the impact of the benthic flux on the water column pH versus DO relationship, we separated benthic flux into "Net-Aerobic" and "Non-Aerobic" parts. As defined in Section 2.2, "Net-Aerobic" flux is the sum of aerobic respiration and re-oxidation of reduced species generated from anaerobic processes (Canfield et al., 1993). The "Net-Aerobic" part of benthic respiration could be integrated with the water column aerobic respiration, because they share the same amount of DIC addition and TA removal ratio with every mole of DO consumption (at a ratio of 106/−17/−138). This is effectively the practice adopted in the earlier analysis by Cai et al. (2011). "Non-Aerobic" part, that is, the net anaerobic respiration and possible $CaCO_3$ dissolution, was defined as the difference between observed flux and "Net-Aerobic" part. Thus, the net impact of benthic respiration on pH versus DO or Ω versus DO curve depends on the "Non-Aerobic" part (Table 3), which alters water column DIC and TA concentrations but not DO concentration. The "Non-Aerobic" part of the TA/DIC ratio (Table 3), in August 2016 and August 2011, was 0.5 and 0.9, respectively. Both ratios were less than the ratio in bottom water (~1.2). The lower benthic "Non-Aerobic" TA/DIC ratio in August 2016 led to a stronger decrease in the TA/DIC ratio in bottom water. Consequently, stronger pH and Ω declines were predicted by the sediment simulation model with August 2016 benthic flux (Figure 4, green line).

In summary, the combination of "Net-Aerobic" and "Non-Aerobic" fluxes can increase the benthic TA/DIC ratio from the Redfield ratio of −17/106 to a positive and reasonably high value (<1), which is still lower than the TA/DIC under low bottom water O_2 conditions. Selectively using one benthic flux under a particular DO concentration can either underestimate or overestimate the benthic impact on bottom pH and Ω changes. However, the current limited sediment flux observations summarized in Table 2 are not sufficient to derive an empirical equation to reliably predict benthic TA/DIC ratio because most early studies did not report benthic TA flux. To overcome this limitation, we illustrated two cases in Figure 4 with two benthic DO flux scenarios (−13.8 versus −5.1 mmol m^{-2} d^{-1}). In other words, instead of exploring a single realistic scenario, our strategy was to estimate the possible ranges of benthic respiration impact on bottom water pH and Ω changes (Figures 4a and 4c). Overall, ΔpH values caused by observed benthic DO, DIC, and TA fluxes were smaller than the range (up to 0.2) reported by Hu et al. (2017), where a TA/DIC ratio of 0.25 derived from a global model was applied. Laurent et al. (2018) used a coupled physical-biogeochemical model and also found extra pH declines in low-DO conditions (Figure 4b in Laurent et al., 2018). However, their

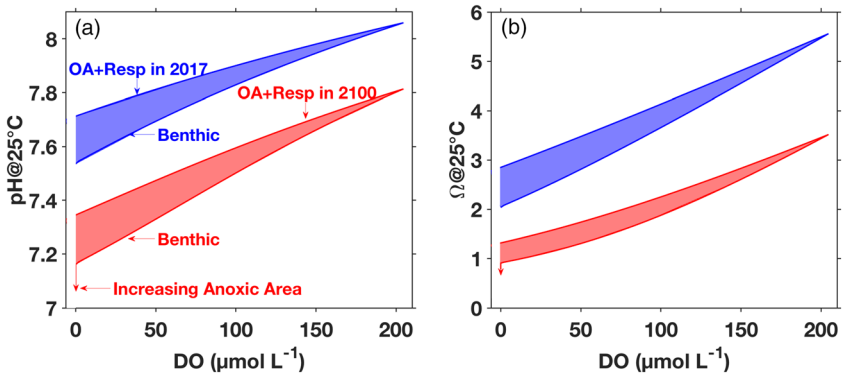

Figure 6. Relationships between (a) pH, (b) Ω, and DO in summer bottom water of the northern Gulf of Mexico. Relationships are calculated for present (year 2017, blue) and future (year 2100 or 800 ppm xCO_2, red) simulations. The shaded areas are the impact of benthic respiration on bottom pH. The vertical red arrow along DO = 0 shows the impact of 10 days of anoxic condition on bottom water (a) pH and (b) Ω. pH changes due to increasing atmospheric CO_2 intrusion, organic carbon aerobic respiration, and observed benthic processes are marked as OA, Resp, and Benthic in panel a. All notes are applicable to Ω change in panel b. Note that we used August 2016 benthic flux (Non-Aerobic benthic TA and DIC ratio is 0.5) to simulate pH and Ω change under the future scenario.

additional pH declines were only due to the weaker buffering capacity of acidified waters because they did not have anaerobic TA flux included in the benthic parameterization.

The novelty of our study was to demonstrate how the benthic anaerobic process, especially, the "Non-Aerobic" fraction impacts bottom water OA. We also found that the benthic respiration did not substantially change the bottom water pH until the year-integrated area reaching around 1.5×10^6 km^2 yr^{-1} (Figure 5), which is reasonable because "Net-Aerobic" respiration is still the dominant process in surface sediment under moderate low bottom water O_2 conditions. The ΔpH and ΔΩ values will become clear only under severe hypoxic and anoxic conditions, when "Non-Aerobic" respiration becomes dominant. This is likely also happening in other coastal oceans that suffer seasonal or persistent hypoxic conditions. Clearly, further study is needed to develop a more comprehensive picture of benthic respiration products under different DO conditions to better refine and constrain future OA dynamics.

4.2. Implication for Future Coastal Bottom Water Ocean Acidification

Models by Laurent et al. (2018) predicted that time-integrated hypoxic area will increase by ~26% in the Gulf of Mexico by 2100 because of the decreasing oxygen solubility and increasing stratification caused by climate change. Our study demonstrates that as the time-integrated extent of hypoxia increases in the Gulf of Mexico, the accumulation of benthic respiration products is favored, leading to greater declines in pH and Ω in 2100 than previously predicted by anthropogenic CO_2 intrusion and organic carbon aerobic respiration (Figure 6).

The increased duration of severe hypoxia and anoxia (Laurent et al., 2018; Lehrter et al., 2017) under a future climate scenario can further decrease bottom pH and Ω. The simulation based on August 2016 (Figure 4a, green dash line) indicates that an additional 10 days of anoxic conditions will result in further pH and Ω decline from 7.57 to 7.41 and 2.20 to 1.58, respectively (at DO = 0, Figures 4a and 4c). This prediction shows the importance of anoxic duration on pH and Ω decreases again because of the accumulation of benthic DIC and TA in bottom water. The exact amount of ΔpH and ΔΩ values by 2100 is difficult to predict because of unknown riverine nutrient and organic matter loading and subsequent impacts on waters and sediment processes in 2100. However, we suggest here that the future ΔpH and ΔΩ values caused by sediment respiration would be higher than the current values under the hypoxic conditions, or even the maximum declines, which is 0.14 (or 0.90). These decreases are compounded by the expected pH (or Ω) decrease of 0.47 (or 2.2) due to water column aerobic respiration, anthropogenic CO_2 increase in the atmosphere and their synergistic effects (Cai et al., 2011). Even though bottom water Ω is still expected to be above 1 in the coming few decades, the dissolution threshold (Ω ~ 1) would occur sooner in bottom hypoxic waters than expected from the combined impact from anthropogenic CO_2 intrusion and organic carbon aerobic respiration

(Figure 6). These potential future conditions of dissolved oxygen conditions in the northern Gulf of Mexico, however, do not include scenarios of increased storminess and increased tropical storm frequency, both of which would breakdown stratification, if even temporarily.

5. Conclusion

Based on a 10-year dataset of summer time inorganic carbonate chemistry, we found that beyond the known acidification effects from anthropogenic CO_2 uptake and aerobic respiration, bottom water pH and Ω have further decreased because of the benthic "Non-Aerobic" respiration, which is positively related to decreased bottom DO concentration. The extensive and prolonged hypoxic or anoxic conditions can amplify the benthic effects on bottom pH and Ω decreases. The extra pH and Ω declines can be alleviated only if the modeled annual time-integrated hypoxic area is well under control (i.e., $<1.5 \times 10^6$ km^2 yr^{-1} in the nGoM). Similar decreases in pH and Ω are likely happening to other shallow bottom water systems that are experiencing eutrophication, such as Chesapeake Bay and Pearl River estuary. This study adds another mechanism to the larger picture linking eutrophication and bottom water OA. In short, benthic respiration, as a eutrophication legacy, can futher enhance bottom water OA.

Data Availability Statement

Data from 2010 to 2017 are publicly available through the Gulf of Mexico Research Initiative Information and Data Cooperative (GRIIDC) at https://data.gulfresearchinitiative.org (UDIs: R3.x164.000:0001, R2.x220.000:0001, R2.x220.000:0002, R2.x220.000:0003, R2.x220.000:0004, R2.x220.000:0005, R2.x220.000:0007, and R2.x220.000:0008) and Biological and Chemical Oceanography Data Management Office (BCO-DMO, https://doi.org/10.1575/1912/bco-dmo.772513.2). All inorganic carbon species in this manuscript can be downloaded from BCO-DMO with link https://www.bco-dmo.org/dataset/818773 (https://doi.org/10.26008/1912/bco-dmo.818773.1). The ROMS simulation of oxygen in the northern Gulf of Mexico from 2005 to 2018 has been archived in Zenodo repository (https://zenodo.org/record/4022853#.X2AE2GdKiF0, https://doi.org/10.5281/zenodo.4022853).

Acknowledgments
We thank Xinping Hu for sharing with us the 2010–2016 data. We acknowledge the support from NSF Chemical Oceanography Program (OCE 0752110, OCE 1559279, and OCE 1756815 to W.-J. Cai, OCE 1756788 to K. Maiti, OCE 1760747 to J. Lehrter, and OCE 1559312 to N. Rabalais), the Gulf of Mexico Research Initiative (RFP-II, GoMRI-020 to W.-J. Cai and X. Hu), and NOAA Grant Nos. NA09NOS4780204 and NA16OAR4320199 (to N. Rabalais).

References

Berelson, W. M., McManus, J., Severmann, S., & Rollins, N. (2019). Benthic fluxes from hypoxia-influenced Gulf of Mexico sediments: Impact on bottom water acidification. *Marine Chemistry*, *209*, 94–106. https://doi.org/10.1016/j.marchem.2019.01.004

Borges, A. V., & Gypens, N. (2010). Carbonate chemistry in the coastal zone responds more strongly to eutrophication than ocean acidification. *Limnology and Oceanography*, *55*(1), 346–353. https://doi.org/10.4319/lo.2010.55.1.0346

Breitburg, D., Levin, L. A., Oschlies, A., Grégoire, M., Chavez, F. P., Conley, D. J., et al. (2018). Declining oxygen in the global ocean and coastal waters. *Science*, *359*(6371), eaam7240. https://doi.org/10.1126/science.aam7240

Brewer, P. G., & Peltzer, E. T. (2016). Ocean chemistry, ocean warming, and emerging hypoxia: Commentary. *Journal of Geophysical Research: Oceans*, *121*, 3659–3667. https://doi.org/10.1002/2016JC011651

Cai, W.-J., Chen, F., Powell, E. N., Walker, S. E., Parsons-Hubbard, K. M., Staff, G. M., et al. (2006). Preferential dissolution of carbonate shells driven by petroleum seep activity in the Gulf of Mexico. *Earth and Planetary Science Letters*, *248*(1–2), 227–243. https://doi.org/10.1016/j.epsl.2006.05.020

Cai, W.-J., Hu, X., Huang, W.-J., Murrell, M. C., Lehrter, J. C., Lohrenz, S. E., et al. (2011). Acidification of subsurface coastal waters enhanced by eutrophication. *Nature Geoscience*, *4*(11), 766–770. https://doi.org/10.1038/NGEO1297

Cai, W.-J., Huang, W.-J., Luther, G. W., Pierrot, D., Li, M., Testa, J., et al. (2017). Redox reactions and weak buffering capacity lead to acidification in the Chesapeake Bay. *Nature Communications*, *8*(1), 369. http://doi.org/10.1038/s41467-017-00417-7

Cai, W.-J., Luther, G. W., Cornwell, J. C., & Giblin, A. E. (2010). Carbon cycling and the coupling between proton and electron transfer reactions in Aquatic Sediments in Lake Champlain. *Aquatic Geochemistry*, *16*, 421–446. https://doi.org/10.1007/s10498-010-9097-9

Cai, W.-J., & Reimers, C. E. (1993). The development of pH and pCO_2 microelectrodes for studying the carbonate chemistry of pore waters near the sediment-water interface. *Limnology and Oceanography*, *38*, 1776–1787. https://doi.org/10.4319/lo.1993.38.8.176

Cai, W.-J., & Sayles, F. L. (1996). Oxygen penetration depths and fluxes in marine sediments. *Marine Chemistry*, *52*(2), 123–131. https://doi.org/10.1016/0304-4203(95)00081-X

Canfield, D. E., Jørgensen, B. B., Fossing, H., Glud, R., Gundersen, J., Ramsing, N. B., et al. (1993). Pathways of organic carbon oxidation in three continental margin sediments. *Marine Geology*, *113*(1–2), 27–40. https://doi.org/10.1016/0025-3227(93)90147-N

Dell'Anno, A., Mei, M. L., Pusceddu, A., & Danovaro, R. (2002). Assessing the trophic state and eutrophication of coastal marine systems: A new approach based on the biochemical composition of sediment organic matter. *Marine Pollution Bulletin*, *44*(7), 611–622. https://doi.org/10.1016/S0025-326X(01)00302-2

Devereux, R., Lehrter, J. C., Beddick, D. L., Yates, D. F., & Jarvis, B. M. (2015). Manganese, iron, and sulfur cycling in Louisiana continental shelf sediments. *Continental Shelf Research*, *99*, 46–56. https://doi.org/10.1016/j.csr.2015.03.008

Devereux, R., Lehrter, J. C., Cicchetti, G., Beddick, D. L., Yates, D. F., Jarvis, B. M., et al. (2019). Spatially variable bioturbation and physical mixing drive the sedimentary biogeochemical seascape in the Louisiana continental shelf hypoxic zone. *Biogeochemistry*, *143*(2), 151–169. https://doi.org/10.1007/s10533-019-00539-8

Dickson, A. G. (1990). Thermodynamics of the dissociation of boric acid in synthetic seawater from 273.15 to 318.15 K. *Deep Sea Research Part A. Oceanographic Research Papers*, *37*(5), 755–766. https://doi.org/10.1016/0198-0149(90)90004-F

Dickson, A. G., & Riley, J. P. (1979). The estimation of acid dissociation constants in sea-water media from potentiometric titrations with strong base. II. The dissociation of phosphoric acid. *Marine Chemistry*, *7*(2), 101–109. https://doi.org/10.1016/0304-4203(79)90002-1

Doney, S. C. (2010). The growing human footprint on coastal and open-ocean biogeochemistry. *Science*, *328*(5985), 1512–1516. https://doi.org/10.1126/science.1185198

Duarte, C. M., Hendriks, I. E., Moore, T. S., Olsen, Y. S., Steckbauer, A., Ramajo, L., et al. (2013). Is ocean acidification an open-ocean syndrome? Understanding anthropogenic impacts on seawater pH. *Estuaries and Coasts*, *36*(2), 221–236. https://doi.org/10.1007/s12237-013-9594-3

Ebner, B. (2019). *Spatiotemporal variation of benthic silica fluxes in the NGOM shelf (Master thesis, #4883)*. Baton Rouge, LA: Louisiana State University. Retrieved from https://digitalcommons.lsu.edu/gradschool_theses/4883

Eldridge, P. M., & Morse, J. W. (2008). Origins and temporal scales of hypoxia on the Louisiana shelf: Importance of benthic and sub-pycnocline water metabolism. *Marine Chemistry*, *108*(3–4), 159–171. https://doi.org/10.1016/j.marchem.2007.11.009

Feely, R. A., Alin, S. R., Newton, J., Sabine, C. L., Warner, M., Devol, A., et al. (2010). The combined effects of ocean acidification, mixing, and respiration on pH and carbonate saturation in an urbanized estuary. *Estuarine, Coastal and Shelf Science*, *88*(4), 442–449. https://doi.org/10.1016/j.ecss.2010.05.004

Feely, R. A., Okazaki, R. R., Cai, W.-J., Bednaršek, N., Alin, S. R., Byrne, R. H., & Fassbender, A. (2018). The combined effects of acidification and hypoxia on pH and aragonite saturation in the coastal waters of the California current ecosystem and the northern Gulf of Mexico. *Continental Shelf Research*, *152*, 50–60. https://doi.org/10.1016/j.csr.2017.11.002

Fennel, K., Hu, J., Laurent, A., Marta-Almeida, M., & Hetland, R. (2013). Sensitivity of hypoxia predictions for the northern Gulf of Mexico to sediment oxygen consumption and model nesting. *Journal of Geophysical Research: Oceans*, *118*, 990–1002. https://doi.org/10.1002/jgrc.20077

Fennel, K., & Testa, J. M. (2019). Biogeochemical controls on coastal hypoxia. *Annual Review of Marine Science*, *11*(1), 105–130. https://doi.org/10.1146/annurev-marine-010318-095138

Gruber, N. (2011). Warming up, turning sour, losing breath: Ocean biogeochemistry under global change. *Philosophical Transactions of the Royal Society of London A: Mathematical, Physical and Engineering Sciences*, *369*(1943), 1980–1996. https://doi.org/10.1098/rsta.2011.0003

Guo, X., Cai, W.-J., Huang, W.-J., Wang, Y., Chen, F., Murrell, M., et al. (2012). Carbon dynamics and community production in the Mississippi River plume. *Limnology and Oceanography*, *57*(1), 1–17. https://doi.org/10.4319/lo.2012.57.1.0001

Hagens, M., Slomp, C., Meysman, F., Seitaj, D., Harlay, J., Borges, A., & Middelburg, J. (2015). Biogeochemical processes and buffering capacity concurrently affect acidification in a seasonally hypoxic coastal marine basin. *Biogeosciences*, *12*(5), 1561–1583. https://doi.org/10.5194/bg-12-1561-2015

Hu, X., & Cai, W.-J. (2011). The impact of denitrification on the atmospheric CO_2 uptake potential of seawater. *Marine Chemistry*, *127*(1–4), 192–198. https://doi.org/10.1016/j.marchem.2011.09.008

Hu, X., Cai, W.-J., Rabalais, N. N., & Xue, J. (2014). Coupled oxygen and dissolved inorganic carbon dynamics in coastal ocean and its use as a potential indicator for detecting water column oil degradation. *Deep Sea Research Part II: Topical Studies in Oceanography*, *129*, 311–318. https://doi.org/10.1016/j.dsr2.2014.01.010

Hu, X., Li, Q., Huang, W.-J., Chen, B., Cai, W.-J., Rabalais, N. N., & Turner, R. E. (2017). Effects of eutrophication and benthic respiration on water column carbonate chemistry in a traditional hypoxic zone in the northern Gulf of Mexico. *Marine Chemistry*, *194*, 33–42. https://doi.org/10.1016/j.marchem.2017.04.004

Huang, W.-J., Cai, W.-J., Wang, Y., Hu, X., Chen, B., Lohernz, S. E., et al. (2015). The response of inorganic carbon distributions and dynamics to upwelling-favorable winds on the northern Gulf of Mexico during summer. *Continental Shelf Research*, *111*, 211–222. https://doi.org/10.1016/j.csr.2015.08.020

Huang, W.-J., Wang, Y., & Cai, W.-J. (2012). Assessment of sample storage techniques for total alkalinity and dissolved inorganic carbon in seawater. *Limnology and Oceanography: Methods*, *10*(9), 711–717. https://doi.org/10.4319/lom.2012.10.711

Jiang, Z. P., Cai, W. J., Chen, B., Wang, K., Han, C., Roberts, B. J., et al. (2019). Physical and biogeochemical controls on pH dynamics in the northern Gulf of Mexico during summer hypoxia. *Journal of Geophysical Research: Oceans*, *124*, 5979–5998. https://doi.org/10.1029/2019JC015140

Kemp, W. M., Sampou, P. A., Garber, J., Tuttle, J., & Boynton, W. R. (1992). Seasonal depletion of oxygen from bottom waters of Chesapeake Bay: Roles of benthic and planktonic respiration and physical exchange processes. *Marine Ecology Progress Series*, *85*, 137–152. https://doi.org/10.3354/meps085137

Krumins, V., Gehlen, M., Arndt, S., Cappellen, P. V., & Regnier, P. (2013). Dissolved inorganic carbon and alkalinity fluxes from coastal marine sediments: Model estimates for different shelf environments and sensitivity to global change. *Biogeosciences*, *10*(1), 371–398. https://doi.org/10.5194/bg-10-371-2013

Laruelle, G. G., Cai, W.-J., Hu, X., Gruber, N., Mackenzie, F. T., & Regnier, P. (2018). Continental shelves as a variable but increasing global sink for atmospheric carbon dioxide. *Nature Communications*, *9*(1), 454. https://doi.org/10.1038/s41467-017-02738-z

Laurent, A., Fennel, K., Cai, W. J., Huang, W. J., Barbero, L., & Wanninkhof, R. (2017). Eutrophication-induced acidification of coastal waters in the northern Gulf of Mexico: Insights into origin and processes from a coupled physical-biogeochemical model. *Geophysical Research Letters*, *44*, 946–956. https://doi.org/10.1002/2016GL071881

Laurent, A., Fennel, K., Ko, D. S., & Lehrter, J. (2018). Climate change projected to exacerbate impacts of coastal eutrophication in the northern Gulf of Mexico. *Journal of Geophysical Research: Oceans*, *123*, 3408–3426. https://doi.org/10.1002/2017JC013583

Lehrter, J., Beddick, D. Jr., Devereux, R., Yates, D., & Murrell, M. (2012). Sediment-water fluxes of dissolved inorganic carbon, O_2, nutrients, and N_2 from the hypoxic region of the Louisiana continental shelf. *Biogeochemistry*, *109*(1–3), 233–252. https://doi.org/10.1007/s10533-011-9623-x

Lehrter, J. C., Ko, D. S., Lowe, L. L., & Penta, B. (2017). Predicted effects of climate change on northern Gulf of Mexico hypoxia. In D. Justić, K. A. Rose, R. D. Hetland, & K. Fennel (Eds.), *Modeling coastal hypoxia: Numerical simulations of patterns, controls and effects of dissolved oxygen dynamics* (pp. 173–214). New York, NY: Springer International Publishing.

Leslie, B. W., Hammond, D. E., Berelson, W. M., & Lund, S. P. (1990). Diagenesis in anoxic sediments from the California continental borderland and its influence on iron, sulfur, and magnetite behavior. *Journal of Geophysical Research*, *95*(B4), 4453–4470. https://doi.org/10.1029/JB095iB04p04453

Liu, X., Patsavas, M. C., & Byrne, R. H. (2011). Purification and characterization of meta-Cresol purple for spectrophotometric seawater pH measurements. *Environmental Science & Technology*, *45*(11), 4862–4868. https://doi.org/10.1021/es200665d

Lueker, T. J., Dickson, A. G., & Keeling, C. D. (2000). Ocean pCO_2 calculated from dissolved inorganic carbon, alkalinity, and equations for K1 and K2: Validation based on laboratory measurements of CO_2 in gas and seawater at equilibrium. *Marine Chemistry*, *70*(1–3), 105–119. https://doi.org/10.1016/S0304-4203(00)00022-0

Morse, J. W., & Eldridge, P. M. (2007). A non-steady state diagenetic model for changes in sediment biogeochemistry in response to seasonally hypoxic/anoxic conditions in the "dead zone" of the Louisiana shelf. *Marine Chemistry*, *106*(1–2), 239–255. https://doi.org/10.1016/j.marchem.2006.02.003

Morse, J. W., & Rowe, G. T. (1999). Benthic biogeochemistry beneath the Mississippi River plume. *Estuaries*, *22*(2), 206–214. http://doi.org/10.2307/1352977

Murrell, M., & Lehrter, J. (2011). Sediment and lower water column oxygen consumption in the seasonally hypoxic region of the Louisiana continental shelf. *Estuaries and Coasts*, *34*(5), 912–924. https://doi.org/10.1007/s12237-010-9351-9

Nunnally, C. C., Rowe, G. T., Thornton, D. C., & Quigg, A. (2013). Sedimentary oxygen consumption and nutrient regeneration in the northern Gulf of Mexico hypoxic zone. *Journal of Coastal Research*, *63*, 84–96. https://doi.org/10.2112/SI63-008.1

Obenour, D. R., Scavia, D., Rabalais, N. N., Turner, R. E., & Michalak, A. M. (2013). Retrospective analysis of midsummer hypoxic area and volume in the northern Gulf of Mexico, 1985–2011. *Environmental Science & Technology*, *47*(17), 9808–9815. https://doi.org/10.1021/es400983g

Rabalais, N. N., Smith, L. M., & Turner, R. E. (2018). The *Deepwater Horizon* oil spill and Gulf of Mexico shelf hypoxia. *Continental Shelf Research*, *152*, 98–107. https://doi.org/10.1016/j.csr.2017.11.007

Rabalais, N. N., Turner, R. E., Gupta, B. K. S., Platon, E., & Parsons, M. L. (2007). Sediments tell the history of eutrophication and hypoxia in the northern Gulf of Mexico. *Ecological Applications*, *17*(sp5), S129–S143. https://doi.org/10.1890/06-0644.1

Rabalais, N. N., Turner, R. E., Sen Gupta, B. K., Boesch, D. F., Chapman, P., & Murrell, M. C. (2007). Hypoxia in the northern Gulf of Mexico: Does the science support the plan to reduce, mitigate, and control hypoxia? *Estuaries and Coasts*, *30*(5), 753–772. https://doi.org/10.1007/BF02841332

Rabalais, N. N., Turner, R. E., & Wiseman, W. J. Jr. (2002). Gulf of Mexico hypoxia, a.k.a. "The Dead Zone". *Annual Review of Ecology and Systematics*, *33*(1), 235–263. https://doi.org/10.1146/annurev.ecolsys.33.010802.150513

Rabalais, N. N., Wiseman, W. J. Jr., & Turner, R. E. (1994). Comparison of continuous records of near-bottom dissolved oxygen from the hypoxia zone along the Louisiana coast. *Estuaries*, *17*(4), 850–861. https://doi.org/10.2307/1352753

Rowe, G. T., Kaegi, M. E. C., Morse, J. W., Boland, G. S., & Briones, E. G. E. (2002). Sediment community metabolism associated with continental shelf hypoxia, northern Gulf of Mexico. *Estuaries*, *25*(6), 1097–1106. https://doi.org/10.1007/BF02692207

Salisbury, J., Green, M., Hunt, C., & Campbell, J. (2008). Coastal acidification by rivers: A threat to shellfish? *Eos, Transactions of the American Geophysical Union*, *89*(50), 513–513. https://doi.org/10.1029/2008EO500001

Smith, V. H. (2003). Eutrophication of freshwater and coastal marine ecosystems a global problem. *Environmental Science and Pollution Research*, *10*(2), 126–139. https://doi.org/10.1065/espr2002.12.142

Turner, R. E., & Rabalais, N. N. (1994). Coastal eutrophication near the Mississippi river delta. *Nature*, *368*(6472), 619–621. https://doi.org/10.1038/368619a0

Turner, R. E., Rabalais, N. N., & Justić, D. (2008). Gulf of Mexico hypoxia: Alternate states and a legacy. *Environmental Science & Technology*, *42*(7), 2323–2327. http://doi.org/10.1021/es071617k

Turner, R. E., Rabalais, N. N., & Justić, D. (2017). Trends in summer bottom-water temperatures on the northern Gulf of Mexico continental shelf from 1985 to 2015. *PLoS ONE*, *12*(9), e0184350. https://doi.org/10.1371/journal.pone.0184350

Uppström, L. R. (1974). The boron/chlorinity ratio of deep-sea water from the Pacific Ocean. *Deep Sea Research and Oceanographic Abstracts*, *21*(2), 161–162. https://doi.org/10.1016/0011-7471(74)90074-6

Van Cappellen, P., & Wang, Y. (1996). Cycling of iron and manganese in surface sediments; A general theory for the coupled transport and reaction of carbon, oxygen, nitrogen, sulfur, iron, and manganese. *American Journal of Science*, *296*(3), 197–243. https://doi.org/10.2475/ajs.296.3.197

Van Dam, B. R., & Wang, H. (2019). Decadal-scale acidification trends in adjacent North Carolina estuaries: Competing role of anthropogenic CO_2 and riverine alkalinity loads. *Frontiers in Marine Science*, *6*(136). https://doi.org/10.3389/fmars.2019.00136

van Heuven, S., Pierrot, D., Rae, J. W. B., Lewis, E. & Wallace, D. W. R. (2011). *MATLAB program developed for CO_2 system calculations*. Oak Ridge, TN. https://doi.org/10.3334/CDIAC/otg.CO2SYS_MATLAB_v1

Wallace, R. B., Baumann, H., Grear, J. S., Aller, R. C., & Gobler, C. J. (2014). Coastal ocean acidification: The other eutrophication problem. *Estuarine, Coastal and Shelf Science*, *148*, 1–13. https://doi.org/10.1016/j.ecss.2014.05.027

Wang, H., Hu, X., Cai, W.-J., & Sterba-Boatwright, B. (2017). Decadal fCO_2 trends in global ocean margins and adjacent boundary current-influenced areas. *Geophysical Research Letters*, *44*, 8962–8970. https://doi.org/10.1002/2017GL074724

Wang, H., Hu, X., Rabalais, N. N., & Brandes, J. (2018). Drivers of oxygen consumption in the northern Gulf of Mexico hypoxic waters—A stable carbon isotope perspective. *Geophysical Research Letters*, *45*, 10,528–10,538. https://doi.org/10.1029/2018GL078571

Wiseman, W. J. Jr., Rabalais, N. N., Turner, R. E., & Justić, D. (2004). Hypoxia and the physics of the Louisiana coastal current. In J. C. J. Nihoul, P. O. Zavialov, & P. P. Micklin (Eds.), *Dying and dead seas, NATO Advanced Research Workshop, Liège, Belgium, NATO ASI Series* (pp. 359–372). Netherlands: Kluwer Academic Publishers. https://doi.org/10.1007/978-94-007-0967-6_15

Woosley, R. J., Millero, F. J., & Takahashi, T. (2017). Internal consistency of the inorganic carbon system in the Arctic Ocean. *Limnology and Oceanography: Methods*, *15*(10), 887–896. https://doi.org/10.1002/lom3.10208

Yu, L., Fennel, K., Laurent, A., Murrell, M., & Lehrter, J. (2015). Numerical analysis of the primary processes controlling oxygen dynamics on the Louisiana shelf. *Biogeosciences*, *12*(7), 2063–2076. https://doi.org/10.5194/bg-12-2063-2015

Zhao, J., Feng, X., Shi, X., Bai, Y., Yu, X., Shi, X., et al. (2015). Sedimentary organic and inorganic records of eutrophication and hypoxia in and off the Changjiang Estuary over the last century. *Marine Pollution Bulletin*, *99*(1–2), 76–84. https://doi.org/10.1016/j.marpolbul.2015.07.060

Zimmerman, A. R., & Canuel, E. A. (2000). A geochemical record of eutrophication and anoxia in Chesapeake Bay sediments: Anthropogenic influence on organic matter composition. *Marine Chemistry*, *69*(1–2), 117–137. https://doi.org/10.1016/S0304-4203(99)00100-0